Journal of Metals, Materials and Minerals, Vol. 32, No. 1, pp. 41-47, 2022

Effect of Al addition on crystal structure of AlGaN/GaN on GaAs (001) substrate grown by metalorganic vapor phase epitaxy

Nattamon SUWANNAHARN[1], Sakuntam SANORPIM[2,*], Suphakan KIJAMNAJSUK[3], Visittapong YORDSRI[3], Noppadon NUNTAWONG[4], and Kentaro ONABE[5]

[1] *Nanoscience and Technology Program, Graduate School, Chulalongkorn University, Pathumwan, Bangkok, 10330, Thailand*
[2] *Department of Physics, Faculty of Science, Chulalongkorn University, Pathumwan, Bangkok, 10330, Thailand*
[3] *National Metal and Materials Technology Center, Thailand Science Park, Klong Luang, Pathumthani, 12120, Thailand*
[4] *National Electronics and Computer Technology Center, Thailand Science Park, Klong Luang, Pathumthani, 12120, Thailand*
[5] *Department of Advanced Material Science, The University of Tokyo, Kashiwanoha, Chiba 277-8561, Japan*

***Corresponding author e-mail:** sakuntam.s@chula.ac.th

Received date:
1 September 2021
Revised date
30 October 2021
Accepted date:
22 November 2021

Keywords:
III-N Semiconductor;
Crystal Structure;
X-ray Diffraction;
TEM;
MOVPE

Abstract

Effects of Al addition on a structural phase modification in AlGaN/GaN films on GaAs (001) substrate grown by MOVPE have been investigated. To examine the effect of Al addition, AlGaN/GaN films were grown with varied a molar flow ratio of TMAl to the total group-III elements of 0, 0.15, and 0.30. Quantity of hexagonal phase incorporation was evaluated by the ratios of integrated XRD intensity of hexagonal $(10\bar{1}1)$ plane to cubic (002) plane from reciprocal space mappings. The diffraction geometry factor was considered in the calculation. The results suggest that GaN primarily contains a hexagonal phase with a small fraction of a cubic phase (15%). With Al addition, a hexagonal phase inclusion significantly decreased. The fraction of a cubic phase becomes dominant (66%) and overcomes a hexagonal phase inclusion. As a result, with an addition of Al, our result demonstrates a structural phase modification from hexagonal to cubic phases in the AlGaN/GaN films on GaAs (001). Besides, TEM image and selective area diffraction patterns indicated that the structural phase might transform through stacking faults. Moreover, the area of the flat surface seen from AFM images indicated a cubic (002) plane, therefore, can briefly comparatively predict the amount of cubic phase in the AlGaN/GaN films.

1. Introduction

GaN and its alloys are very high potential semiconductor materials extensively applied in electronic and optoelectronic applications for these current decades. Moreover, GaN-based material is enabled to engineer a bandgap energy and lattice parameter by making ternary and quaternary alloys [1] with other III-N semiconductor materials, i.e., InN or/and AlN [2]. This ability of bandgap energy and lattice parameter tailoring offers new spectral regions from approximately 0.7 eV (InN) to 3.5 eV (GaN), and 6.2 eV (AlN) [3]. In the literature, there are a considerable number of studies on bandgap engineering and structural modifications of materials with Al substitution [4-6]. For group III-Nitride semiconductors, the Al element is contained in the ternary or quaternary alloys, e.g., AlGaN, AlGaInN, for making the quantum well structure with a desirable bandgap [7] or tailoring bandgap for designing high-efficiency and high-brightness white light-emitting diodes (LEDs) [8]. In carbon-based materials, Al-doping provides superior improvement of adsorption capacity for drug delivery function due to its lowest binding energy, as well as enhance the non-linear optical properties, e.g., dipole moment, mean static polarizability and anisotropic polarizability. So far, it has been utilized in the hexagonal phase. But, the limitation of employing a hexagonal phase is the polarization due to its absence of symmetry, which degrades the radiative recombination efficiency [9]. Recently, the cubic phase is also crystallized and exhibits superior properties, e.g., small Auger recombination loss [10], high electron mobility [11], and hole mobility [12]. In addition, it is symmetrical results in internal polarization free, which leads to higher radiative recombination efficiency [13,14]. Accordingly, a cubic GaN and its ternary alloys namely AlGaN/GaN heterostructures become applicable in many devices applications, for example, MODFETs [15], photodetector [16], etc.

However, a cubic phase structure is not easily be synthesized because of its metastability and lack of suitable substrate. As a consequence, it transforms to a hexagonal phase. Therefore, a hexagonal phase inclusion is inevitable, and its amount becomes substantial with increasing film thickness, result in degraded cubic crystal quality [17]. But, there is a numerical study reported that the structural phase transition from hexagonal phase to cubic phase could occur in AlGaN with high Al composition [18].

Therefore, in this study, AlGaN/GaN was grown on GaAs (001) substrate by MOVPE with different Al addition by changing a molar

flow ratio of the Al precursor to the total group-III elements. The effect of Al addition on structural phase modification in AlGaN/GaN films was determined. Reciprocal space mapping (RSM) utilizing high-resolution X-ray diffraction (HRXRD) and micro-Raman spectroscopy were performed to assess the volume of cubic and hexagonal phase inclusion in AlGaN/GaN films. Cross-sectional transmission electron microscopy (TEM) images, as well as the selective area diffraction (SAD) patterns, were obtained to examine the structural phase transformation. Besides, atomic force microscopy (AFM) images were employed to determine the relationship between the amount of hexagonal phase inclusion and the surface morphology. Also, scanning electron microscopy (SEM) was performed to determine a morphology of cross-section as well as a nominal thickness.

2. Experimental

AlGaN/GaN films used in this study were grown on GaAs (001) substrates by low-pressure (160 Torr) MOVPE. Trimethylaluminum (TMAl), trimethylgallium (TMGa), dimethylhydrazine (DMHy) and tertiarybutylarsine (TBAs) were used as the precursors of Al, Ga, N, and As, respectively. Substrate preparation was firstly done by deposition of GaAs buffer layer at 650°C for 10 min, or approximately 100 nm, to provide a smoother surface. The second step was to deposit the GaN low-temperature buffer layer at 575°C for 2 min, or approximately 20 nm, to also smoothen a substrate interface. Besides, it serves as a protection layer for GaAs from thermal decomposition at high-temperature growth and acts as nucleation of GaN.

Then, three samples with different Al addition were grown at 900°C. The Al addition was varied by changing the molar flow ratio (x_v) of TMAl to the total group-III elements (TMAl + TMGa), $x_v = \frac{[TMAl]}{[TMAl]+[TMGa]}$ For the first sample, GaN layer was grown for 15 min, followed by the AlGaN main layer with x_v of 0.15 for 30 min. For the second sample, after the growth of GaN layer, the AlGaN main layer with x_v of 0.30 was grown for 30 min. Lastly, for the third sample, the GaN layer was grown for 30 min without TMAl injected. The nominal thickness of the three samples measured from the cross-sectional SEM images was 1.5 μm, 1.3 μm and 2.0 μm for the first, second and third samples, respectively.

The crystal structure of AlGaN/GaN films was assessed by micro-Raman spectroscopy with an excitation wavelength of 532.5 nm, as well as HRXRD with Cu-$K_{\alpha 1}$ wavelength of 1.5406 Å in $2\theta/\omega$ scan and RSM modes. The RSMs of each sample were recorded from two specific rotation angles at [110] and [1$\bar{1}$0] directions, which denote as ϕ_0 and ϕ_{90}, respectively. Besides, the azimuth angles (ω) were also varied from -10 degrees to 10 degrees, where $\Delta\omega$ was an angle with respect to a cubic (002) plane. Moreover, an AFM was used to probe the surface morphology, and transmission electron microscopy was performed at an accelerating voltage of 200 kV including energy-dispersive X-ray spectroscopy.

3. Results and discussion

The crystal structure of the AlGaN/GaN films with different Al compositions was first analyzed using micro-Raman spectroscopy. Concentration of Al was defined by the vapor phase composition of group-III precursors, x_v of 0, 0.15, 0.30, where $x_v = \frac{[TMAl]}{[TMAl]+[TMGa]}$ as mentioned in the experimental section. Figure 1 shows Raman frequencies corresponding to the phonon modes of cubic and hexagonal GaN crystals. The Lorentzian line-shape was well-fitted to the Raman spectra including the cubic GaN related transverse optical (TO) phonon and longitudinal optical (LO) phonon modes located at 550.3±1.1 cm^{-1} and 737.7±0.5 cm^{-1}, respectively. In addition, the E_2 (high) phonon mode at 567.7±0.1 cm^{-1} corresponding to a hexagonal GaN was also well fitted with the Lorentzian line-shape. Therefore, this primarily confirms the coexistence of cubic and hexagonal phases in the samples. As illustrated in Figure 1, a hexagonal E_2 (high) phonon mode was much stronger than a cubic LO phonon mode in the GaN film without Al addition, $x_v = 0$, whereas the hexagonal E_2 (high) phonon mode in the AlGaN/GaN films with x_v = 0.15 and 0.30 was comparable to a cubic LO phonon mode. However, these were the qualitative measurement and could not indicate how much each phase included because the phonon frequency was also affected by other factors such as the defect, strain, thickness etc.

In contrast, to evaluate Al composition (x) in $Al_xGa_{1-x}N$, it can be estimated as a function of A_1(LO) or E_2(high) phonon frequency [19,20]. In this experiment, E_2 (high) phonon frequency in AlGaN has expected to blue shift due to compressive stress induced as the Al composition increases. But the shift of E_2 (high) cannot be observed. This might be due to a small amount of the Al content incorporated in the AlGaN film. The obstacle to achieving the AlGaN with high Al composition is a common problem, known as the parasitic reaction, in Figure 1 which the precursor of Nitrogen and Aluminum interact with each other to become adducts and prevent the deposition of AlGaN onto the substrate [21,22]. As a consequence, the efficiency of the Al incorporation is limited and difficult to control [23]

Before examining the volume of hexagonal and cubic phase in AlGaN/GaN films, the $2\theta/\omega$ scan was performed to probe the orientation of the growth of cubic and hexagonal AlGaN/GaN paralleled to the horizontal plane and expressed in Figure 2. X-ray diffraction

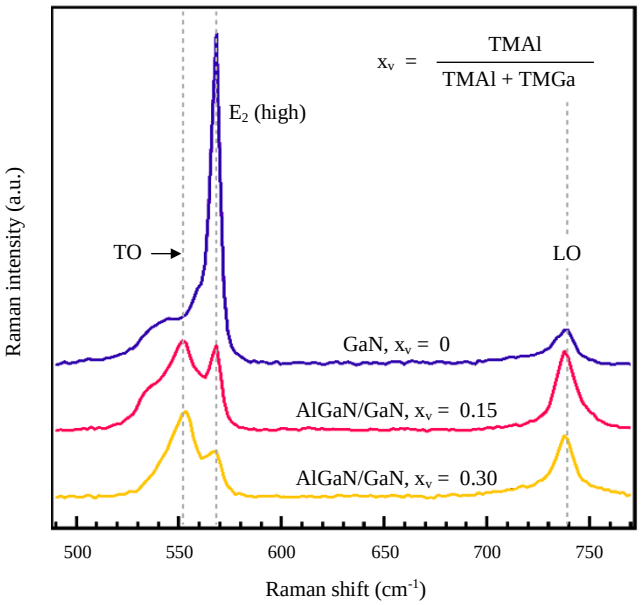

Figure 1. Raman spectra reveal the coexistence of cubic and hexagonal phase in AlGaN/GaN films with varied Al addition (x_v = 0, 0.15 and 0.30).

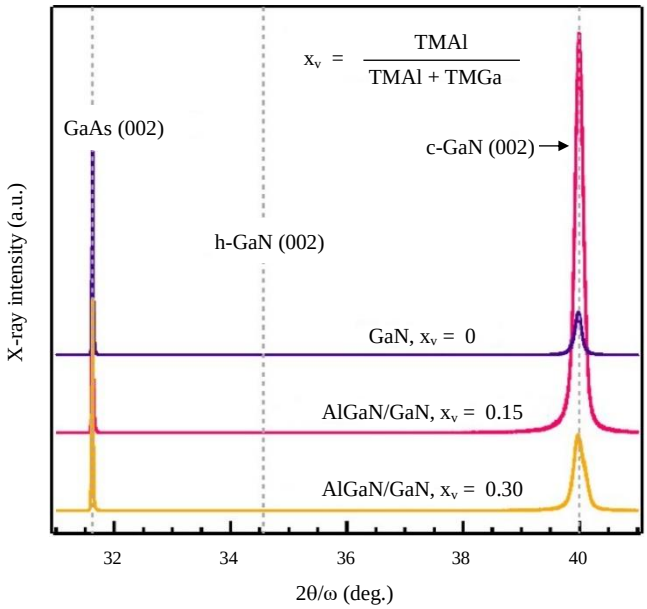

Figure 2. HRXRD (002) 2θ/ω scans for AlGaN/GaN films with varied Al addition (x_v = 0, 0.15 and 0.30).

from a (002) plane of cubic GaN is observed at 2θ/ω of 40.0 degrees for the GaN film without Al addition (the third sample), whereas the (002) diffraction peak from AlGaN films with x_v = 0.15 (the first sample) and 0.30 (the second sample) is still not clearly resolved due to a low Al concentration in AlGaN films. However, diffraction from a hexagonal (0002) at 2θ/ω of 34.6 degrees is not observed as detected by micro-Raman spectroscopy. It can be indicated that a hexagonal (0002) plane, in this study, does not parallel to a cubic (002) plane. Besides, X-ray intensity diffracted from GaAs (002) was normalized to compare intensities diffracted from cubic (002). It is seen that AlGaN/GaN film with x_v = 0.15 provides the highest intensity of cubic (002), and another AlGaN/GaN film with x_v = 0.30 exhibits a similar trend to the intensity of LO phonon mode in Raman spectra displayed in Figure 1.

Additionally, even though neither Raman spectra nor X-ray diffraction profiles of AlGaN could be resolved to examine a solid Al composition (x), the energy-dispersive X-ray spectroscopy (EDX) equipped with TEM was performed for elemental analysis. The EDX results suggested that the AlGaN with x_v = 0.15 and 0.30 contained solid Al composition of 3.0±1.0 at% ($Al_{0.03}Ga_{0.97}N$) and 8.0±1.0 at% ($Al_{0.08}Ga_{0.92}N$), respectively. Additionally, the effectiveness of the Al incorporation in the growth of the $Al_{0.03}Ga_{0.97}N$ (x = 3.0±1.0 at%) and $Al_{0.08}Ga_{0.92}N$ (x = 8.0±1.0 at%) films with x_v= 0.15 and 0.30, respectively, can be determined using $x = \frac{p\cdot[TMAl]}{p\cdot[TMAl]+[TMGa]}$ [22], assuming that TMGa was completely consumed. Where *p* is a factor reflected a depletion of TMAl during the growth, indicating an incorporation efficiency of Al into the film. Accordingly, the *p* factor was evaluated to be 0.18 (18%) and 0.20 (20%) in the samples with x_v of 0.15 and 0.30, respectively. This means that, in our work, a large amount of TMAl might become the adduct due to parasitic reaction, while only 18% to 20% could be incorporated into AlGaN film. The solid Al composition (x) in $Al_xGa_{1-x}N$ analyzed by EDX was listed in Table 1.

To quantitatively determine the volume of hexagonal phase inclusion in cubic AlGaN/GaN or vice versa with different Al addition, the HRXRD was performed since the X-ray intensity can identify the quantity of crystalline volume (V_{phase}) of interest, as stated in Equation 1. Relationship between the volume of a cubic and hexagonal phases and their X-ray diffraction intensities can be summarized by Equation 2 and 3, respectively. I_o is the incident X-ray intensity, F_{hkl} is the structure factor which includes the temperature factor resulting from thermal vibration and diffraction angle, *LP* and *M* is the Lorentz-polarization and multiplicity factor, respectively, V_{cell} is the volume of the unit cell, *AG* is an absorption factor, which integrated over the thickness of the film with diffraction geometry correction, e^{-2d} is the temperature factor, and V_{phase} is the irradiated crystalline volume of the structural phase of interest.

$$I = I_o \cdot \left(\frac{|F|}{V_{cell}}\right)^2 \cdot LP \cdot M \cdot e^{-2d} \cdot AG \cdot V_{phase} \quad (1)$$

As it is known that a hexagonal phase inclusion in GaN favors developing on cubic (111) plane, which means hexagonal (0002) plane parallel to cubic (111) plane. For this orientation, a cubic (002) and hexagonal $(10\bar{1}1)$ planes can be detected using RSM. RSM measurements were done at two rotation angles paralleled to [110] and $[1\bar{1}0]$, denoted as ϕ_0 and ϕ_{90}, respectively, for extensive detection of hexagonal developed on cubic {111} planes. Figure 3 demonstrates a presence of hexagonal $(10\bar{1}1)$ diffraction peaks at Δω of ±7.2 degrees as seen in RSMs, confirming a construction of hexagonal inclusion on cubic (111) plane. As seen in Figure 3(c-f) and their insets, the elliptical shape of diffraction peaks elongating along the 2θ/ω axis relating to a cubic (002) at 2θ/ω of 40.0 degrees was observed due to the overlapping of the diffraction from cubic (002) GaN and cubic (002) AlGaN with a smaller lattice constant and small amount of Al incorporation. Due to a higher Al incorporation in AlGaN/ GaN film with x = 8.0±1.0 at% (x_v = 0.30), the shoulder of diffraction peak of cubic (002) AlGaN/GaN, as see an inset in Figure 3(e), is more clear observable, compared to that of the film with x = 3.0±1.0 at% (x_v = 0.15). Therefore, we integrated this bundled diffraction from both GaN and AlGaN to evaluate the overall cubic and hexagonal phase in AlGaN/GaN films.

Table 1. The weighting factor, α, of hexagonal to cubic phase without and with diffraction geometry correction for the AlGaN/GaN films with varied Al addition and thickness. Thickness was determined by cross-sectional SEM images.

x_v	*x*	Thickness (μm)	Without geometry diffraction correction	With geometry diffraction correction	
			α	α^-	α^+
0	0	2.0	1.07	1.82	0.82
0.15	0.03±0.01 (3.0±1.0 at%)	1.5	1.07	1.84	0.83
0.30	0.08±0.01 (8.0±1.0 at%)	1.3	1.07	1.85	0.83

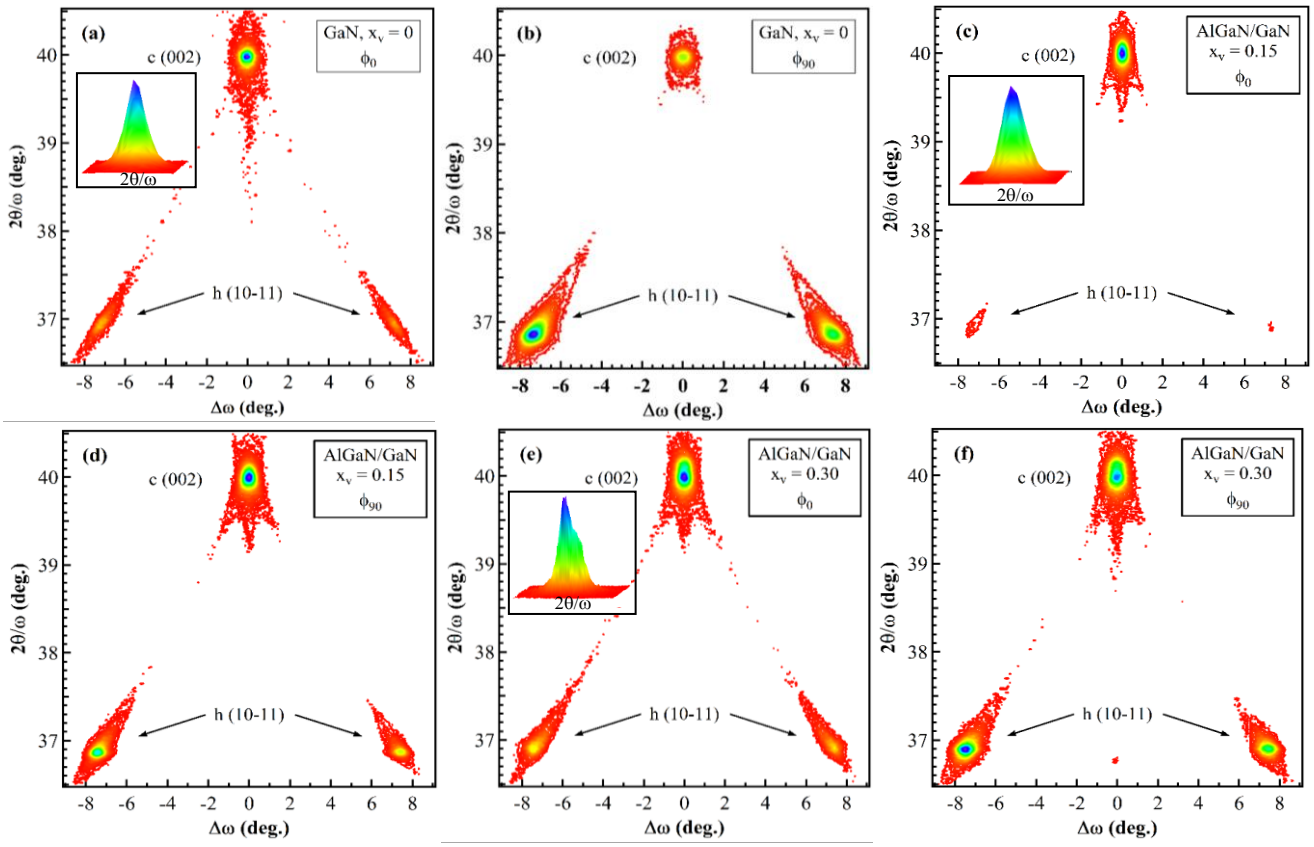

Figure 3. Reciprocal space mapping of AlGaN/GaN with varied Al addition (x_v= 0, 0.15 and 0.30).

$$V_c = \frac{I_c}{I_0} \cdot \frac{V_{cell,c}^2}{|F_c|^2 \cdot LP_c \cdot M_c \cdot AG_c} \quad (2)$$

$$V_h = \frac{I_h}{I_0} \cdot \frac{V_{cell,h}^2}{|F_h|^2 \cdot LP_h \cdot M_h \cdot AG_h} \quad (3)$$

$$AG^{\pm} = \int_0^t \frac{e^{-\mu x\left(\frac{1}{\sin(\theta+\Delta\omega)} \pm \frac{1}{\sin(\theta-\Delta\omega)}\right)}}{\sin(\theta \pm \Delta\omega)} dx \quad (4)$$

$$\frac{V_h^{\pm}}{V_c} = \frac{1}{\alpha^-} \cdot \frac{\sum I_h}{I_c} + \frac{1}{\alpha^+} \cdot \frac{\sum I_h^+}{I_c} \quad (5)$$

$$\frac{1}{\alpha^{\pm}} \equiv \frac{V_{cell,h}^2}{|F_h|^2 \cdot LP_h \cdot M_h \cdot AG_h^{\pm}} \cdot \frac{|F_c|^2 \cdot LP_c \cdot M_c \cdot AG_c^{\pm}}{V_{cell,c}^2} \quad (6)$$

Moreover, it is seen from all RSMs that the X-ray intensity diffracted from hexagonal $(10\bar{1}1)$ measured at Δω = -7.2 degrees is higher than the intensity measured at Δω = +7.2 degrees. This is due to asymmetrical measurement. In general, a larger irradiated area of the X-ray beam exposed to the sample at negative angles of Δω, resulted in a higher X-ray diffraction intensity, whereas a smaller irradiated area at positive angles of Δω reflected a lower X-ray diffraction intensity. Consequently, diffraction geometry correction was recognized in the absorption factor in this study to improve the calculation by taking 2θ, Δω, and path length into account as expressed in Equation 4, instead of $e^{-2\mu t}$ without geometry correction. The superscript +, -, represents the geometry of measurement at positive Δω and negative Δω, respectively. Hence, the ratio of hexagonal phase volume to cubic phase volume can be evaluated using Equation 5, where the ensemble of diffraction factors was shortened as α^- and α^+ as in Equation 6.

Table 1 presents a hexagonal to cubic phase volume calculation for the AlGaN/GaN films with different Al addition using α with and without diffraction geometry correction. Without diffraction geometry correction, α in this study was estimated to be 1.07 which is nearly equivalent to the theoretical value calculated in another published research (1.06) [24]. With diffraction geometry correction, α^- is in a range of 1.82-1.85, while α^+ vary from 0.82-0.83, depending on the thickness of the samples.

In Table 2, the integrated X-ray diffraction intensities and amount of hexagonal phase inclusion in the AlGaN/GaN films with varied Al addition were summarized. The amount of hexagonal phase inclusion in the AlGaN/GaN films with x = 0, 3.0±1.0 at% (x_v = 0.15), and 8.0±1.0 at% (x_v = 0.30) was calculated to be 85%, 34%, and 53%, respectively. The results suggest that when Al was added by injecting the TMAl precursor with x_v = 0.15, a hexagonal phase inclusion drastically drops from 85% to 34%, which means that a cubic phase becomes dominant of 66%. Moreover, when x_v is increased up to 0.30, a hexagonal phase inclusion moderately drops from 85% to 53%. This reveals that Al addition effects the structural modification form hexagonal phase to cubic phase. Reduction of hexagonal phase inclusion in the AlGaN/GaN film with x_v = 0.30 is not as expected since it may be affected by the parasitic reaction. As noticed in Table 1, the lower nominal thickness of the AlGaN/GaN film with x_v = 0.30 compared to the film with x_v = 0.15 indicates a consequence of the severe effect of parasitic reaction when TMAl flow rate increases [23]. This may also affect the potency of structural phase transition.

Table 2. Integrated X-ray diffraction intensities (in arbitrary unit) and amount of hexagonal phase inclusion for the AlGaN/GaN films with varied Al addition.

x_v	α^-	α^+	I_c^*	ϕ_0		ϕ_{90}		$\sum_{\phi_{0,90}} \frac{V_h^{\pm}}{V_c}$	$\%V_h$	$\%V_c$
				I_h^-	I_h^+	I_h^-	I_h^+			
0	1.82	0.82	96,031	21,372	13,925	430,138	226,929	5.664	85%	15%
0.15	1.84	0.83	96,031	3,827	1,844	44,054	17,624	0.516	34%	66%
0.30	1.85	0.83	96,031	23,266	15,911	68,590	34,413	1.148	53%	47%

I_c^* is normalized I_c

To further investigate the structural phase modification, a bright-field transmission electron microscopy (TEM) image in the [110] zone axis was illustrated in Figure 4(a). The dark line with an inclination angle of 54.7 degrees associate with the stacking faults (SFs) where a cubic phase can transform into a hexagonal phase and vice versa due to their structural similarity. Selective-area diffraction (SAD) pattern obtained from the region near the interface between film and substrate, namely region A, exhibits the three patterns including a face-centered cubic (FCC), and a hexagonal close-packed (HCP) in two orientations. These two orientations of HCP patterns verify that a hexagonal phase develops on the cubic {111} planes. Moreover, the SAD pattern took close to the top surface which parallels to the horizontal plane (region B) exhibits the FCC pattern, whereas close to the top incline surface presents the HCP pattern. As a result, it may be concluded that a cubic plane contributes to the flat surface morphology, while a hexagonal plane provides an inclined surface morphology. Also, it is consistent with the X-ray measurements in Figure 2 that a hexagonal (0002) plane is not observed paralleled to the horizontal plane, but a cubic (002). Accordingly, AFM images in Figure 5 show the extensive surface morphology to verify the assumption. It is seen that the AlGaN/GaN film with $x_v = 0.15$ (Figure 5(b)) which contains 66% of cubic phase reveals a more area of flat surface than the AlGaN/GaN film with $x_v = 0.30$ (Figure 5(c)). On the other hand, GaN without Al addition contained 15% of a cubic phase mainly presents the inclined surface. It can be said that a flat surface morphology can briefly demonstrate cubic phase in the AlGaN/GaN films.

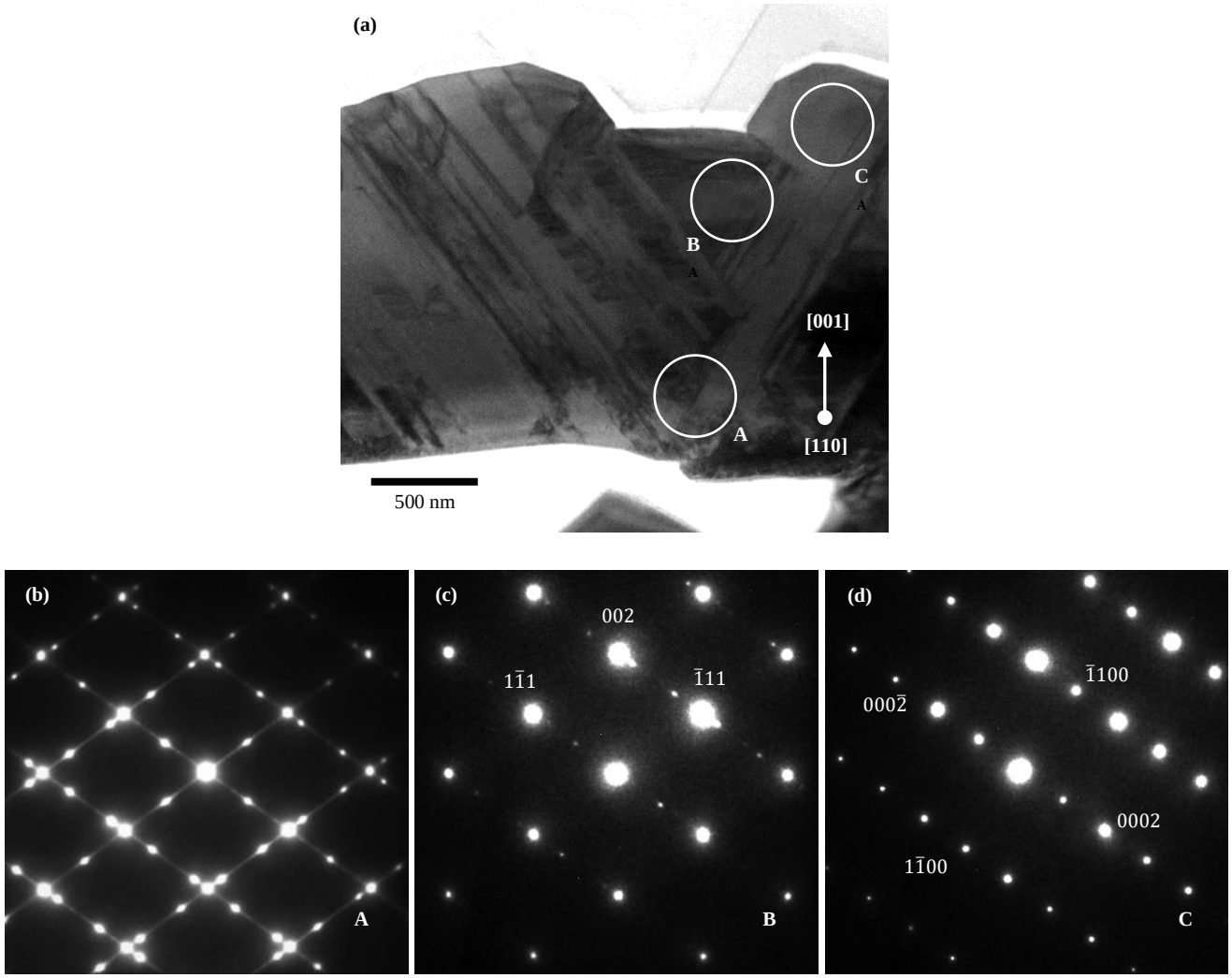

Figure 4. (a) TEM micrograph of AlGaN/GaN film with the highest cubic purity (x=3.0±1.0 at%) along [110] zone axis, and (b-d) selective area diffraction pattern in three specific regions indicated by circles.

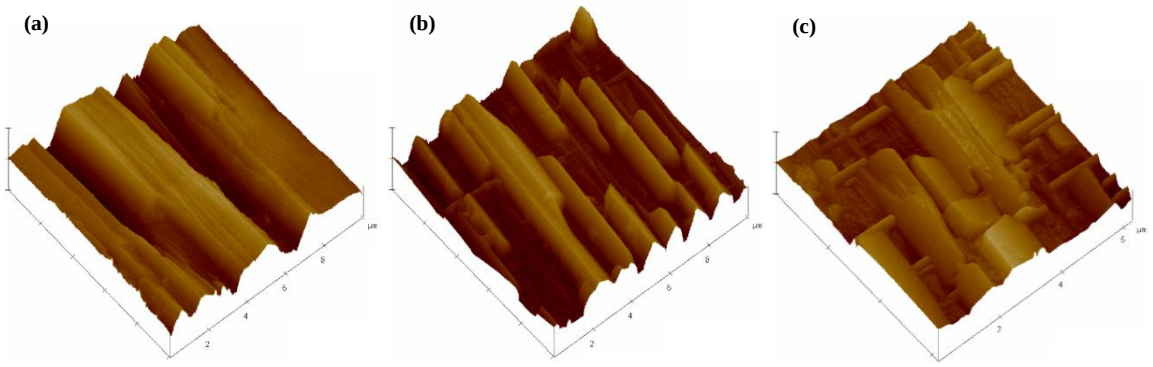

Figure 5. AFM images presented the surface morphology of AlGaN/GaN with x_v of (a) 0, (b) 0.15, and (c) 0.30.

4. Conclusions

Raman spectra preliminarily confirm the polytype of hexagonal and cubic in the AlGaN/GaN films. Without Al addition, integrated X-ray diffraction intensity from cubic (002) and hexagonal ($10\bar{1}1$) plane indicates that GaN contains a high fraction of hexagonal phase of 85%. With the Al addition, even if a parasitic reaction affected the incorporation of Al, the AlGaN/GaN films successfully presents a much smaller fraction of a hexagonal phase. The molar flow ratio (x_v) of TMAl to the total group-III elements (TMAl + TMGa) of 0.15 provides the lowest amount of hexagonal phase of 34%, and a cubic phase becomes dominant with the purity of 66%. A higher molar flow ratio, x_v=0.30, provides a moderate reduction of hexagonal phase to 53%. Therefore, it can be concluded that the presence of TMAl supports a modification of a structural phase from hexagonal to cubic phase. Moreover, TEM images and SAD patterns indicate the structural phase transformation through stacking faults, and the area of flat surface contributes to the cubic domain. Thus, the amount of cubic phase might be comparatively evaluated from the area of flat surface morphology taken from AFM images.

Acknowledgements

This work is supported by the Thailand Research fund (TRF) (Grant number: RSA5480025). The authors acknowledge the 100th Anniversary Chulalongkorn University for Doctoral Scholarship and the Overseas Research Experience Scholarship for Graduate Students for their financial supports.

References

[1] D. S. Patil, *Semiconductor laser diode technology and applications*. IntechOpen, London, 2012.

[2] M. O. Manasreh, *III-Nitride Semiconductors*, "Defects and structural properties," *Elsevier Science*, 2000.

[3] I. Vurgaftman, and J. R. Meyer, "Band parameters for nitrogen-containing semiconductors," *Journal of Applied Physics*, vol. 94, no. 6, pp. 3675-3696, 2003.

[4] İ. Muz, and M. Kurban, "A first-principles evaluation on the interaction of 1,3,4-oxadiazole with pristine and B-, Al-, Ga-doped C60 fullerenes," *Journal* of *Molecular Liquids*, vol. 335, p. 116181, 2021.

[5] M. Kurban, and İ. Muz, "Theoretical investigation of the adsorption behaviors of fluorouracil as an anticancer drug on pristine and B-, Al-, Ga-doped C36 nanotube," *Journal of Molecular Liquids*, vol. 309, p. 113209, 2020.

[6] İ. Muz, and M. Kurban, "A comprehensive study on electronic structure and optical properties of carbon nanotubes with doped B, Al, Ga, Si, Ge, N, P and As and different diameters," *Journal of Alloys* and *Compounds*, vol. 802, pp. 25-35, 2019.

[7] W. Yang, L. Jinchai, L. Wei, L. Shuping, C. Hangyang, L. Dayi, Y. Xu, and K. Junyong, "Control of two-dimensional growth of AlN and high Al-content AlGaN-based MQWs for deep-UV LEDs," *AIP Advances.*, vol. 3, no. 5, p. 052103, 2013.

[8] Y. C. Tsai, and C. Bayram, "Structural and electronic properties of hexagonal and cubic phase AlGaInN alloys investigated using first principles calculations," *Scientific Reports*, vol. 9, no. 1, p. 6583, 2019.

[9] A. der. M. Matthias, P. Alessandro, P. Gabriele, R. Walter, and D. C. Aldo**,** "Efficiency drop in green InGaN/GaN light emitting diodes: The role of random alloy fluctuations," *Physical Review Letters*., vol. 116, no. 2, p. 027401, 2016.

[10] K. T. Delaney, P. Rinke, and C. G. Van De Walle, "Auger recombination rates in nitrides from first principles," *Applied Physics Letters*, vol. 94, no. 19, p. 191109, 2009.

[11] F. Mireles, and S. E. Ulloa, "Acceptor binding energies in GaN and AlN," *Physical Review B*, vol. 58, no. 7, pp. 3879-3887, 1998.

[12] C. G. Rodrigues, J. R. L. Fernandez, J. R. Leite, V. A. Chitta, V. N. Freire, A. R. Vasconcellos, and R. Luzzi, "Hole mobility in zincblende c–GaN," *Journal of Applied Physics.*, vol. 95, no. 9, p. 4914, 2004.

[13] S. Nakamura, and G. Fasol, *The blue laser diode: GaN based light emitters and lasers*. Springer, 1997.

[14] D. Ahn, and S.-H. Park, "Optical gain of strained hexagonal and cubic GaN quantum-well lasers," *Applied Physics Letters*, vol. 69, no. 22, pp. 3303-3305, 1996.

[15] D. Bouguenna, A. Boudghene Stambouli, N. Mekkakia Maaza, A. Zado, and D. J. As, "Comparative study on performance of cubic AlxGa1−xN/GaN nanostructures MODFETs and MOS-MODFETs," *Superlattices* and *Microstructures*, vol. 62, pp. 260-268, 2013.

[16] A. Radosavljević, J. Radovanović, V. Milanović, and D. Indjin, "Cubic GaN/AlGaN based quantum wells optimized for

applications to tunable mid-infrared photodetectors," Optical and *Quantum Electronics*, vol. 47, no. 4, pp. 865-872, 2014.

[17] N. Zainal, S. V. Novikov, A. V. Akimov, C. R. Staddon, C. T. Foxon, and A. J. Kent, "Hexagonal (wurtzite) GaN inclusions as a defect in cubic (zinc-blende) GaN," *Physica B Condened. Matter*, vol. 407, no. 15, pp. 2964-2966, 2012.

[18] D. Cai, and J. Kang, "Thickness-dependent phase transition of AlxGa1-xN thin films on strained GaN," *Journal of Physical Chemistry B*, vol. 110, no. 21, pp. 10396-10400, 2006.

[19] M. Kuball, "Raman spectroscopy of GaN, AlGaN and AlN for process and growth monitoring/control," Surface and Interface *Analysis*, vol. 31, no. 10, pp. 987-999, 2001.

[20] A. Cros, H. Angerer, O. Ambacher, M. Stutzmann, R. Hopler, and T. Metzger, "Raman study of the optical phonon in AlxGa1-xN alloys," *Solid State Communications*, vol. 104, no. 1, pp. 35-39, 1997.

[21] D. G. Zhao, J. J. Zhu, D. S. Jiang, H. Yang, J. W. Liang, X. Y. Li, and H. M. Gong, "Parasitic reaction and its effect on the growth rate of AlN by metalorganic chemical vapor deposition," *Journal of Crystal Growth*, vol. 289, no. 1, pp. 72-75, 2006.

[22] C. H. Chen, H. Liu, D. Steigerwald, W. Imler, C. P. Kuo, M. G. Craford, M. Ludowise, S. Lester, and J. Amano,, "A study of parasitic reactions between NH_3 and TMGa or TMAl," *Journal of Electronic Materials*, vol. 25, no. 6, pp. 1004-1008, 1996.

[23] M. E. Coltrin, J. Randall Creighton, and C. C. Mitchell, "Modeling the parasitic chemical reactions of AlGaN organometallic vapor-phase epitaxy,"*Journal of Crystal Growth*, vol. 287, no. 2, pp. 566-571, 2006.

[24] H. Tsuchiya, K. Sunaba, S. Yonemura, T. Suemasu, and F. Hasegawa, "Cubic Dominant GaN Growth on (001) GaAs Substrates by Hydride Vapor Phase Epitaxy," *Japanese Journal of Applied Physics*, vol. 36, no. Part 2, No. 1A/B, pp. L1-L3, 1997.